Atherosclerosis 281 (2019) 47–55

Contents lists available at ScienceDirect

Atherosclerosis

journal homepage: www.elsevier.com/locate/atherosclerosis

Hematopoietic Stabilin-1 deficiency does not influence atherosclerosis susceptibility in LDL receptor knockout mice

Joya E. Nahon[a], Menno Hoekstra[a,*], Silvia van Hulst[a], Calin Manta[b], Sergij Goerdt[b,c], Janine J. Geerling[a], Cyrill Géraud[b,c,d], Miranda Van Eck[a]

[a] Division of BioTherapeutics, Leiden Academic Centre for Drug Research (LACDR), Gorlaeus Laboratories, Einsteinweg 55, 2333CC, Leiden, the Netherlands
[b] Department of Dermatology, Venereology, and Allergology, University Medical Center and Medical Faculty Mannheim, Heidelberg University, And Center of Excellence in Dermatology, Mannheim, Germany
[c] European Center for Angioscience, Medical Faculty Mannheim, Heidelberg University, Mannheim, Germany
[d] Section of Clinical and Molecular Dermatology, Medical Faculty Mannheim, Heidelberg University, Mannheim, Germany

HIGHLIGHTS

- Scavenger receptor Stabilin-1 deficiency does not alter foam cell formation *in vivo*.
- Bone marrow-specific Stabilin-1 KO does not affect atherosclerosis susceptibility.
- A potential role for Stabilin-1 in metabolic disorders is suggested.

ARTICLE INFO

Keywords:
Atherosclerosis
Bone marrow transplantation
Foam cell
Macrophages
Scavenger receptor

ABSTRACT

Background and aims: Stabilin-1 (STAB1) is a scavenger receptor expressed on alternatively activated macrophages and sinusoidal endothelial cells. Its ligands include oxidized low-density lipoprotein (LDL) and the extracellular matrix glycoprotein SPARC and it is present in both human and murine atherosclerotic lesions. We aimed to investigate the effect of specific deletion of STAB1 in bone marrow-derived cells, including macrophages on atherosclerotic lesion formation in mice.

Methods: Lethally irradiated hypercholesterolemic LDL receptor knockout mice received either wildtype (WT) or *STAB1* knockout (*STAB1* KO) bone marrow. Bone marrow transplanted mice were fed a Western-type diet for 9 weeks to induce atherosclerotic lesion formation.

Results: Interestingly, LDL receptor knockout mice reconstituted with *STAB1* KO bone marrow showed increased body weight gain (two-way ANOVA: $p < 0.001$) and larger white adipocyte cell sizes (43% increase in cell area; $p < 0.05$) as compared to WT bone marrow transplanted mice, which correlated positively ($r = 0.82$; $p < 0.001$). This was paralleled by a significant increase in white adipose tissue relative mRNA expression levels of the adipokine leptin (+94% $p < 0.05$). Despite these changes, no differences in serum lipid levels, the extent of *in vivo* macrophage foam cell formation or circulating leukocyte concentrations were observed. Moreover, the size and composition of atherosclerotic lesions was not different between the two experimental groups.

Conclusions: Bone marrow-specific Stabilin-1 deletion does not affect the susceptibility for atherosclerosis in mice. However, the increased body weight gain and adipocyte cell size highlight a potential role for leukocyte STAB1 in the development of metabolic disorders.

1. Introduction

Scavenger receptors are a group of structurally diverse surface receptors denominated by their ability to recognize a great variety in ligands (reviewed in Van Berkel et al. [1]). These ligands include pathogens, apoptotic cells and modified (e.g. oxidized, glycosylated) lipoproteins. Stabilin-1 (STAB1, FEEL-1, CLEVER-1, MS-1) is a class H scavenger receptor. STAB1 was originally identified by Goerdt and colleagues as MS-1, a scavenger receptor on liver sinusoidal endothelial cells that mediates the uptake of oxidized low-density lipoproteins (oxLDL) [2,3]. In addition to oxLDL, the extracellular matrix glycoprotein secreted protein acidic and rich in cysteine (SPARC) [3,4],

* Corresponding author.
E-mail address: hoekstra@lacdr.leidenuniv.nl (M. Hoekstra).

https://doi.org/10.1016/j.atherosclerosis.2018.12.020
Received 20 July 2018; Received in revised form 2 December 2018; Accepted 5 December 2018
Available online 30 December 2018
0021-9150/

advanced glycosylation end products, pathogens and apoptotic cells are recognized by STAB1, defining it as a true scavenger receptor [5–7]. Besides executing its classical scavenger function in liver sinusoidal endothelial cells, STAB1 on lymphatic endothelial cells facilitates T-lymphocyte transmigration and modulates the angiogenic capacity of human umbilical vein endothelial cells [8,9]. In addition to endothelial cells, STAB1 is expressed in subsets of (tissue) macrophages both under physiological and inflammatory conditions [10,11]. The expression of STAB1 can be upregulated in macrophages by stimulation with interleukin-4 and dexamethasone and is downregulated upon stimulation with interferon-gamma [12]. Interestingly, STAB1 expression is induced both in human atheroma samples as well as in an apolipoprotein E knockout murine model for atherosclerosis, as shown by a combination of tissue microarrays and quantitative immunohistochemistry [13]. In the atheroma samples, STAB1 is expressed both in endothelial cells and in macrophage-rich areas. Furthermore, monocytes, macrophage precursors, circulating in patients with familiar hypercholesterolemia show an increased surface expression of STAB1 [14] and monocyte STAB1 has been shown to have an immune modulatory function [15]. Importantly, STAB1 is highly expressed on M2 macrophages, and M2 macrophages display an increased susceptibility to macrophage foam cell formation [16,17]. On the other hand, macrophage STAB1 is also important for removal of apoptotic cells [6,18] and hence effective efferocytosis to prevent atherosclerotic plaque progression [19]. Based on these combined findings, it can be hypothesized that macrophage STAB1 may play a role in the development of atherosclerotic lesions. In the current study we therefore investigated the impact of bone marrow STAB1 deficiency on the atherogenic process.

2. Materials and methods

2.1. Animals

C57BL/6 and low-density lipoprotein receptor knockout (*LDLr* KO) mice (The Jackson Laboratory, Bar Harbor, ME) were bred in house at the animal facility of the Leiden Academic Centre for Drug Research. Male C57BL/6J and *STAB1* KO donor mice on a C57BL/6J background were bred in house at the Medical Faculty Mannheim of the Ruprecht-Karls University of Heidelberg and maintained at the animal facility of the Leiden Academic Centre for Drug Research until the start of the experiment. The experiment was executed in rooms that were temperature controlled and had a 12h/12h light dark cycle. The mice were kept in sterilized filter-top cages for the duration of the experiment. All animal work was approved by the Dutch Ethics Committee and regulatory authority at Leiden University and was carried out in compliance with Dutch government guidelines and the Directive 2010/63/EU of the European Parliament on the protection of animals used for scientific purposes and complies with the ARRIVE guidelines.

2.2. Stabilin-1 expression under atherogenic conditions

Peritoneal macrophages (PM) were elicited by injecting 1 mL 3% Brewer's thioglycollate medium (Difco, Detroit, MI) into the peritoneal cavity of C57BL/6 mice. Five days after injection, cells were harvested by PBS lavage of the peritoneal cavity. To generate bone marrow-derived macrophages (BMDM), bone marrow cells were isolated from femurs of C57BL/6 mice and cultured for 7 days in complete RPMI medium supplemented with 20% FCS and 30% L929 cell-conditioned medium as a source of macrophage colony-stimulating factor. After harvesting, PM and BMDM were cultured overnight in DMEM containing 10% FCS. Subsequently, cells were loaded with 20 ng/mL oxLDL for 48 h in DMEM containing 0.2% BSA to generate foam cells. A RNAeasy mini kit (Qiagen, Chatsworth, CA) was used to isolate total RNA (N = 3 per group). After checking the concentration and integrity of the RNA and an amplification step (Ambion, #IL1791), the MouseWG-6 v2.0 microarray was performed according to manufacturer's specifications (Illumina, San Diego, CA).

For analysis of the expression of STAB1 in developing lesions, data were used from a microarray dataset acquired by our group, as previously published [20]. In short, bilateral collars were placed around carotid arteries in male *LDLr* KO mice fed a Western-type diet containing 0.25% cholesterol and 0.15% cacao butter (SDS, Sussex, UK) to induce localized atherosclerotic lesion development [21]. RNA was isolated from snap-frozen, pooled carotid arteries that were harvested every two weeks from week 0 to week 10 after induction of atherosclerotic lesion formation. Microarray analysis was performed after processing of the RNA using the Illumina Bead-Chip Whole Genome Microarray platform (ServiceXS). In an independent experiment, these conditions were replicated and RNA was isolated for validation using RT-PCR.

2.3. Bone marrow transplantation

The bone marrow recipient male *LDLr* KO mice were randomized into two groups according to equal age, weight and total and free cholesterol levels and irradiated with two consecutive doses of 4.5 Gy (0.141 Gy/min, 200 kV, 4 mA) using an Andrex Smart 225 Röntgen source (XYLON International, Copenhagen, Denmark) with a 6-mm aluminum filter one day before the bone marrow transplantation. Mice either received bone marrow from wild-type mice (WT) (N = 12) or *STAB1* KO mice on a C57BL/6J background (N = 11). Hereto, femurs and tibia were flushed over a 70-μm cell strainer (Greiner Bio-One, Alphen a/d Rijn, The Netherlands) with PBS to obtain bone marrow in a single cell suspension. 5×10^6 bone marrow cells were injected intravenously into the tail vein of the irradiated mice. The bone marrow transplanted mice were left to recover for nine weeks, during which they received sterilized regular chow diet (Special Diet Services, Witham, Essex, UK). Subsequently, the mice were switched to a Western-type diet containing 15% cocoa butter and 0.25% cholesterol (Special Diet Services, Witham, Essex, UK) to induce the development of atherosclerotic lesions. At nine weeks after the start of the atherogenic diet, mice were anesthetized by a mix of xylazine (70 mg/kg), ketamine (350 mg/kg) and atropine (1.8 mg/kg). Blood was collected via the orbital sinus and peritoneal cells were isolated, after which the mice were perfused with PBS. Heart, spleen, bone marrow and gonadal white adipose tissue were collected. Genomic DNA was isolated from bone marrow using a PureLink® Genomic DNA Mini Kit (Life Technologies, Bleiswijk, The Netherlands). PCR analysis was performed on this genomic DNA using the following *STAB1* primers (Eurogentec S.A., Seraing, Belgium) to confirm hematological chimerism of the transplanted animals (Fig. 1): Forward primer - AGACTATGGTCTCAG TCTGGGA, WT-specific reverse primer – CTGCAATCACTGTCCCCAC ACT, *STAB1* KO-specific reverse primer – TTATTTCATACCCGCCAGTT CTGA.

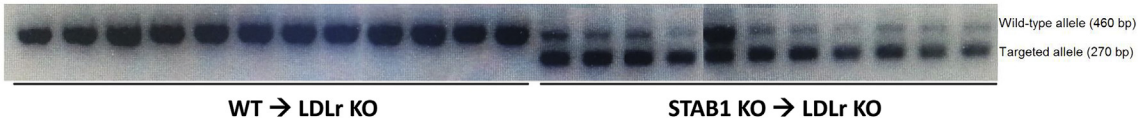

Fig. 1. Successful disruption of STAB1 in bone marrow after transplantation.
PCR on genomic DNA isolated from bone marrow of WT (N = 12) and *STAB1* KO (N = 11) bone marrow transplanted mice at 18 weeks after transplantation.

2.4. Histological analysis

Hearts were fixed for 72 h in 3.7% neutral-buffered formalin (Shandon Formal-Fixx, Thermo scientific, Runcorn, UK) and stored in 0.1% sodiumazide in PBS. Prior to sectioning, hearts were embedded in Tissue-Tek® O.C.T. ™ (Sakura Finetek, Alphen a/d Rijn, The Netherlands) for 24 h. Sections of the aortic root were generated using a CM3050S cryostat (Leica, Rijswijk, The Netherlands) at 10 μm intervals and collected serially. Neutral lipids were stained using Oil red O (Sigma-Aldrich, Zwijndrecht, The Netherlands). Hematoxylin (Sigma-Aldrich) was used to stain nuclei. Masson's Trichrome staining (Sigma-Aldrich) was used to determine collagen content. For the macrophage staining, a primary monoclonal Rat-anti-mouse CD68 antibody (FA-11; ab53444; Abcam, Cambridge, UK) was used after 1:1000 dilution in block buffer. A secondary AP-conjugated goat-anti-rat IgG (A8438, Sigma-Aldrich, Zwijndrecht, The Netherlands) was used at a dilution of 1:100 in block buffer. For detection, the ready-to-use BCIP®/NBT liquid substrate system was used (Sigma-Aldrich, Zwijndrecht, The Netherlands). Mean lesion area (μm^2) was quantified with a Leica DMRE microscope and HC PL FLUOTAR objective, coupled to a video camera using Qwin V3 software (Leica Ltd, Cambridge, UK). Lesion area and collagen content were quantified blinded and started at tricuspid valves in four lipid and collagen stained sections.

White adipose tissue was embedded in paraffin and sectioned using a RM2235 rotary microtome (Leica) at intervals of 5 μm. Sections were stained with hematoxylin and eosin (Merck, Darmstadt, Germany). Adipocyte cell area was quantified using a Leica DMRE microscope and HC PL FLUOTAR objective, coupled to a video camera using Qwin V3 software (Leica Ltd, Cambridge, UK), at magnification 10 × . Qwin V3 software was used to measure the total area of the image. Subsequently, adipocyte cells were manually counted within this area and the adipocyte cell area was determined by dividing the total area by the number of adipocytes counted. Quantification consisted of three sections per mouse. Quantification was performed blinded.

2.5. Plasma lipids

Plasma concentrations of total cholesterol, free cholesterol and triglycerides were determined using enzymatic colorimetric assays as described by Out et al. [22]. The cholesterol distribution over the different lipoproteins was determined per group by fractionation of 30 μL of pooled plasma using a Superose 6 column (3.2 × 300 mm, Smartsystem, Pharmacia, Uppsala, Sweden) to perform fast protein liquid chromatography.

2.6. Hematological analysis

Hematological analysis was performed on blood and peritoneal cells using an XT-2000i Automated Hematology Analyzer (Sysmex Corporation, Etten-Leur, The Netherlands) to measure leukocyte counts/concentrations. The percentage of peritoneal foam cells was determined based upon their distinct localization in the Sysmex scatterplots, as previously described [23]. After lysis of erythrocytes using ACK lysis buffer, leukocyte populations were determined by flow cytometry in blood samples and splenocyte suspensions using a BD FACS Canto II (BD Biosciences, San Jose, CA). FACS antibodies were acquired from BioLegend (San Diego, CA), BD Biosciences (San Jose, CA), and ThermoFisher Scientific (Waltham, MA). FlowJo software (Flowjo,Lcc/BD Biosciences, San Jose, CA) was used to identify monocytes (CD11b + Ly6G-), neutrophils (CD11b + Ly6G+), B-cells ($CD19^+$) and T-cells (CD3+/CD4+ and CD3+/CD8+). CCR2 and Ly6C were included in the flow cytometry panels as monocyte activation markers, while Ki67 was applied as lymphocyte proliferation marker.

2.7. RT-PCR

RNA was isolated using the guanidium thiocyanate/phenol/chloroform extraction method according to Chomczynski and Sacchi [24] and reverse transcribed by RevertAid Reverse Transcriptase (Life Technologies). Relative gene expression was measured using SYBR Green Technology (Eurogentec, Maastricht, The Netherlands) on an ABI PRISM 7500 Taqman apparatus (Applied Biosystems, Bleiswijk, The Netherlands). Primers were validated for identical efficiencies. Primer sequences are available upon request. Beta-actin (*ACTB*), glyceraldehyde-3-phosphate dehydrogenase (*GAPDH*), ribosomal protein L27 (*RPL27*), and acidic ribosomal phosphoprotein P0 (*36B4*) were used as reference genes.

2.8. Statistical analysis

Statistical analysis was performed using Graphpad Prism (GraphPad Software, La Jolla, California, USA). Results are depicted as means ± SEM or individual data points with the average displayed as a horizontal line. Student's two-tailed t-tests or a two-way ANOVA with a Bonferroni test for multiple comparisons were used to compare the data of two normally distributed groups. Welch's correction was used to correct for unequal variances and outliers were detected by a Grubbs' test. Spearman correlation coefficient was calculated using Prism software (GraphPad Software, La Jolla, California, USA). A probability value of $p < 0.05$ was considered significant.

3. Results

Previous findings by Brochériou et al. have suggested that the expression of STAB1 is increased during atherosclerotic lesion development [13]. As evident from Fig. 2A, we also detected a higher gene expression of STAB1 in diseased arteries as compared to non-atherosclerotic arteries. Upon induction of atherosclerotic lesion formation, the aortic expression of STAB1 was markedly increased as compared to STAB1 expression at baseline (270% increase after two weeks; $p < 0.001$, Fig. 2A). When taking into account the aortic expression profile of the macrophage marker CD68 during lesion formation [25], and that STAB1 expression is generally lower in inflammatory monocyte/macrophages as compared to their non-inflammatory (resident) counterparts [15,26], it is anticipated that the increase in STAB1 expression is probably driven by the infiltration of monocytes that are subsequently converted into STAB1-expressing macrophages. Notably, after the initial macrophage infiltration phase, aortic STAB1 expression was reduced from week 4 onwards to a level that was still somewhat higher than that at baseline (Fig. 2A). These results were validated in an independent experiment under similar experimental conditions using RT-PCR to measure STAB1 expression (data not shown). In accordance with the notion that macrophage STAB1 expression is reduced during *in vivo* macrophage foam cell formation and lesion progression, exposure to the foam cell-inducing agent oxLDL decreased *STAB1* gene expression both in BMDM (37% decrease; $p < 0.05$; Fig. 2B) and PM (53% decrease; $p < 0.01$; Fig. 2C).

Bone marrow transplantation into hyperlipidemic mice is a well-established model to investigate the atherogenic potential of genes expressed in monocytes and macrophages [27]. To uncover a potential contribution of monocyte/macrophage STAB1 to the pathogenesis of atherosclerosis, the effect of bone marrow-specific *STAB1* deletion on atherosclerotic lesion formation was investigated in *LDLr* KO mice on a Western-type diet. Body weight was monitored regularly during the course of the experiment. Surprisingly, after the transient irradiation-induced drop in body weight, *STAB1* KO transplanted mice gained more weight as compared to WT transplanted mice (two-way ANOVA: $p < 0.001$; Fig. 3A). In parallel, the white adipocyte cell area was increased in adipose tissue of *STAB1* KO transplanted mice (43% increase; $p < 0.05$; Fig. 3B and C). White adipocyte cell area correlated

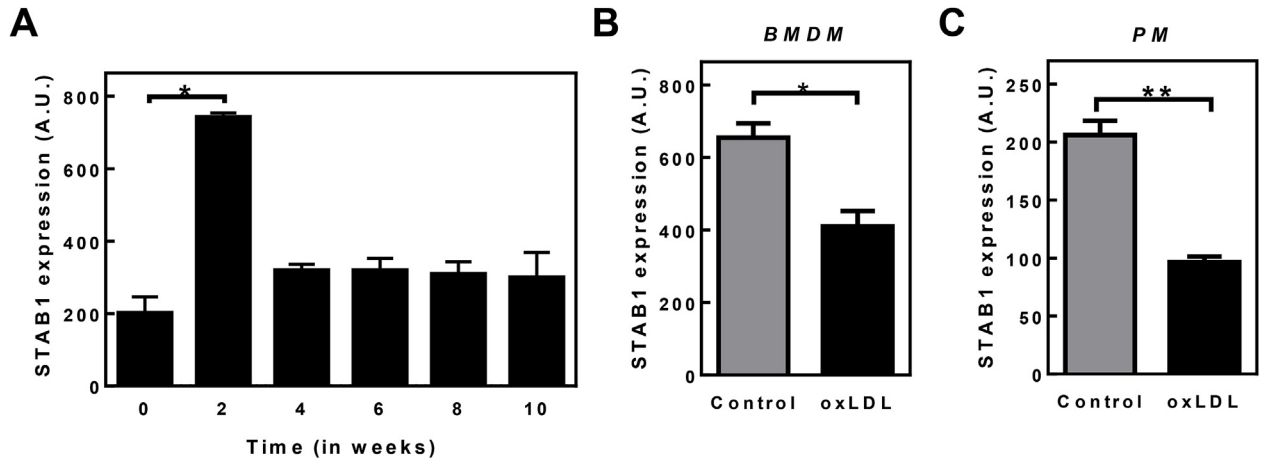

Fig. 2. Expression of STAB1 is modulated under atherogenic conditions.
(A) During initiation of atherosclerotic lesion in the first two weeks of lesion development, STAB1 is increased as compared to baseline. During the progression of the lesion, STAB1 values are almost normalized. Graphs represent means ± SEM (N = 3). Loading with oxLDL (black bars) reduced the relative gene expression of *STAB1* in bone marrow-derived macrophages (BMDM; B) and in thioglycollate-elicited peritoneal macrophages (PM; C) as compared to control macrophages (grey bars). $*p < 0.05$ $**p < 0.01$.

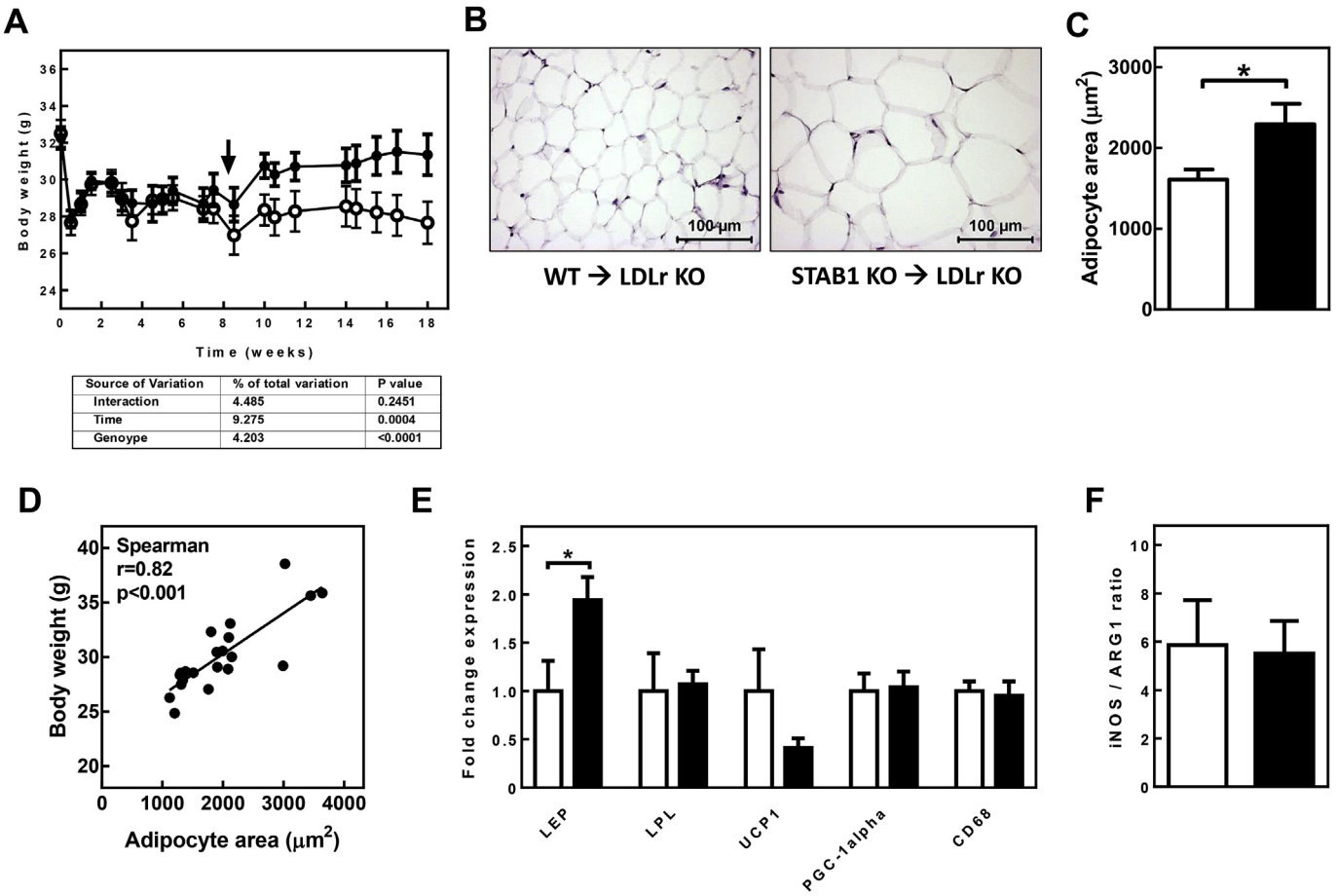

Source of Variation	% of total variation	P value
Interaction	4.485	0.2451
Time	9.275	0.0004
Genoype	4.203	<0.0001

Fig. 3. Total body weight is affected by bone marrow-specific STAB1 deletion in *LDLr* KO mice as a result of changes in the white adipose tissue.
(A) *STAB1* KO transplanted *LDLr* KO mice (black circles; N = 11) gained more weight as compared to WT transplanted control mice (white circles; N = 12). The arrow indicates the start of Western-type diet feeding. (B) Representative micrographs of white adipose tissue at 20× magnification. (C) Adipocyte cell area was significantly increased in *STAB1* KO transplanted mice (black bar; N = 11) as compared to control WT transplanted mice (white bar; N = 12). (D) Body weight and adipocyte cell area correlated significantly. (E) White adipose tissue gene expression of leptin (LEP) but not that of lipolysis (LPL), browning (UCP-1/PGC-1alpha) or macrophage (CD68) markers was significantly increased in *STAB1* KO transplanted mice (black bar; N = 10) as compared to WT transplanted mice (white bar; N = 9). (F) The ratio between the expression of M1 and M2 macrophage markers iNOS and ARG1 in white adipose tissue was similar in the two experimental groups. Graphs represent means ± SEM. $*p < 0.05$.

significantly with body weight (r = 0.82; $p < 0.001$; Fig. 3D), indicating that this might be causal for the change in body weight. In further support of a more obese phenotype, the relative gene expression of the obesity-associated adipokine leptin (LEP) was significantly increased in white adipose tissue of *STAB1* KO transplanted mice as compared to WT transplanted controls (124% increase; $p < 0.01$; Fig. 3E). The increase in adiposity extent was not due to an increased lipolytic activity of the white adipose tissue, as judged from the similar expression level of lipoprotein lipase (LPL; Fig. 3E). No apparent browning was morphologically visible in white adipose tissue sections of both types of recipient mice. In accordance, expression of the brown adipose tissue markers uncoupling protein 1 (UCP1) and peroxisome proliferator-activated receptor gamma co-activator-1alpha (PGC-1alpha) could almost not be reliably detected in white adipose tissue specimens and was not significantly different between the two bone marrow genotypes (Fig. 3E). Inflammation in adipose tissue, i.e. infiltration of pro-inflammatory macrophages, and the formation of crown-like structures have been linked to adipocyte (dys)function and the development of obesity-related metabolic complications such as insulin resistance and diabetes [28]. In accordance with early stage adiposity, crown-like structures could rarely be found in white adipose tissue of both groups of transplanted mice (data not shown). In addition, expression levels of the macrophage marker CD68 were virtually identical in white adipose tissue samples of *STAB1* KO transplanted mice and WT transplanted controls (Fig. 3E). Importantly, no change was observed in the adipose tissue expression ratio of the M1 macrophage-type marker inducible nitric oxide synthase (iNOS) and the M2 macrophage-type marker arginase 1 (ARG1) (Fig. 3F), suggesting that the polarization state of the infiltrated macrophages and the associated inflammatory potential of these immune cells were also not different in the two experimental groups.

Despite the apparent difference in body weight development, plasma free and total cholesterol as well as triglyceride levels were not significantly different between *STAB1* KO transplanted and control WT transplanted animals (Fig. 4A). The distribution of cholesterol over the different lipoprotein classes was also similar between both experimental groups (Fig. 4B).

Peritoneal leukocytes were isolated and the relative amount of macrophage foam cells was analyzed as a measure of *in vivo* foam cell formation. Despite the function of STAB1 as a macrophage scavenger receptor for modified lipoproteins, bone marrow-specific STAB1 deficiency was only associated with a trend towards a decrease in the extent of foam cell formation (41% decrease; $p = 0.07$; Fig. 5A and B). Real-time RT-PCR was used to identify possible compensatory changes in the expression of other receptors involved in macrophage lipoprotein uptake. Stabilin-2 (STAB2), a scavenger receptor showing 55% homology with STAB1 on protein level, was not expressed at a level that could be reliably detected in either WT or *STAB1* KO peritoneal leukocyte fractions. *LDLr* and very low-density lipoprotein receptor (*VLDLr*) gene expression was also virtually absent. The scavenger receptors A1 (SR-A1), B—I (SR-BI) and CD36 were present but their relative mRNA expression levels were not significantly different between *STAB1* KO transplanted mice and WT transplanted controls (Fig. 5C).

Since STAB1 has been implicated in the immune response [8,15], we measured the effect of bone marrow STAB1 deficiency on circulating leukocytes. Total circulating leukocyte numbers were not significantly different between *STAB1* KO transplanted and WT transplanted mice (Fig. 6A). In support of this, flow cytometric analysis showed that the percentages of monocytes, neutrophils, B-lymphocytes and T-lymphocytes in the circulation were not different (Fig. 6B). Notably, the percentage of monocytes highly expressing the activation/infiltration markers Ly6C and CCR2 was also similar in blood of the two types of bone marrow recipients (61 ± 3% for *STAB1* KO *versus* 61 ± 4% for WT; $p > 0.05$). *STAB1* KO transplanted mice also had a comparable splenocyte profile as WT transplanted control mice (Fig. 6C). In accordance with the notion that hematopoietic STAB1 deficiency did not have a relevant effect on lymphocyte homeostasis, the bone marrow genotype did not significantly impact the percentages of splenic $CD4^+$ helper T-cells and $CD8^+$ cytotoxic T-cells expressing the proliferation marker Ki67 (13 ± 1% and 20 ± 2% *versus* 15 ± 1% and 19 ± 1% for WT, respectively; $p > 0.05$).

The extent of atherosclerosis was determined in the aortic root. As evident from Fig. 7A, both groups of mice displayed significant lesion development after nine weeks of atherogenic Western-type diet feeding. *LDLr* KO mice transplanted with WT bone marrow exhibited average aortic root lesions of 171 ± $23*10^3$ μm^2 that almost fully consisted of macrophages, as judged from the CD68 staining (Fig. 7A). As it can be appreciated from Fig. 7A and B, *STAB1* KO bone marrow transplanted mice also contained macrophage-rich early lesions that did not differ in size (253 ± $39*10^3$ μm^2; $p = 0.08$) as compared to WT transplanted mice. The lesional amount of collagen, analyzed by Masson's Trichrome staining of the aortic root sections, was also similar in the *STAB1* KO transplanted and WT transplanted mice (Fig. 7A and C).

4. Discussion

We aimed to uncover whether macrophage STAB1 contributes to atherosclerotic lesion formation in mice. Here we show that bone

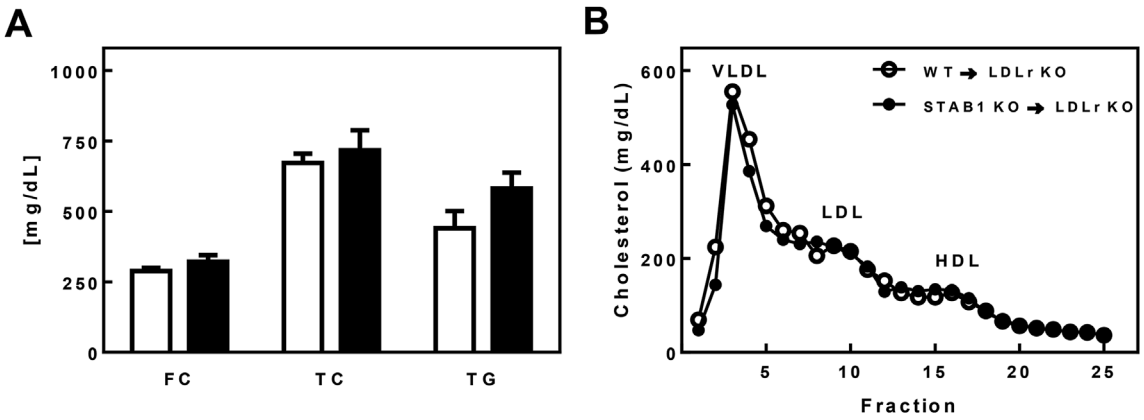

Fig. 4. Plasma lipids are not changed after bone marrow-specific *STAB1* deletion in *LDLr* KO mice.
(A) Levels of free cholesterol (FC), total cholesterol (TC) and triglycerides (TG) were not different between the *STAB1* KO bone marrow transplanted group (black bars; N = 11) and the WT transplanted group (white bars; N = 12) after 9 weeks of Western-type diet feeding. (B) The distribution of cholesterol over the lipoprotein fractions was not different in the *STAB1* KO transplanted group (black circles; N = 3) as compared to the WT transplanted group (white circles; N = 3). Graphs represent means ± SEM.

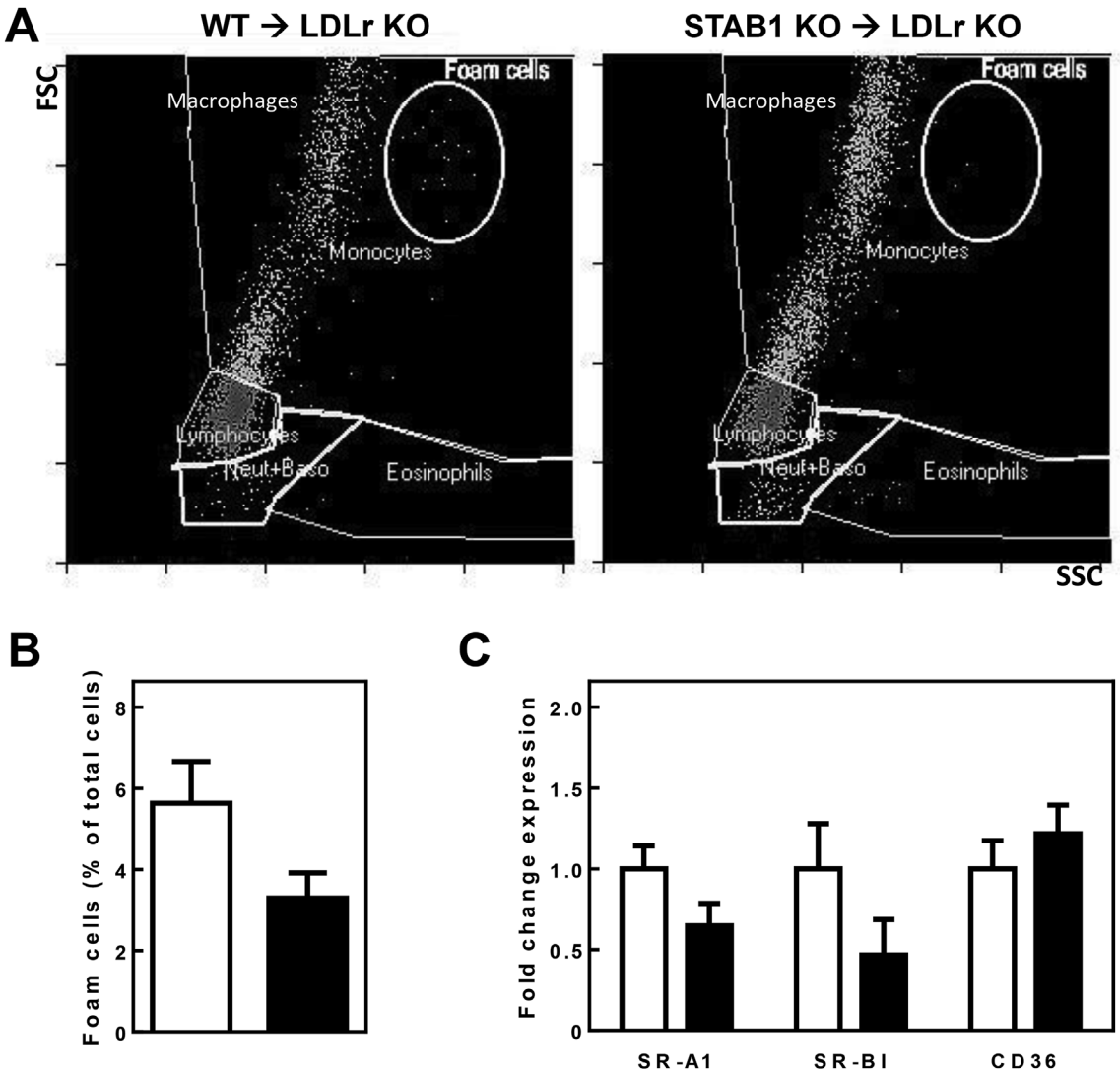

Fig. 5. Bone marrow specific *STAB1* deletion in *LDLr* KO mice does not affect *in vivo* foam cell formation.
(A) Representative scatterplots of the different leukocyte populations in the peritoneal cavity. The gate for SSC^{high}/FSC^{high} foam cells is indicated with a circle. (B) The percentage foam cells of the total peritoneal leukocyte population did not differ between *STAB1* KO transplanted (black bar; N = 11) and WT transplanted mice (white bar; N = 12). (C) Relative expression of uptake receptors in the peritoneal leukocyte population of *STAB1* KO transplanted (black bars; N = 5) as compared to those of WT transplanted mice (white bars; N = 6). Graphs represent means ± SEM.

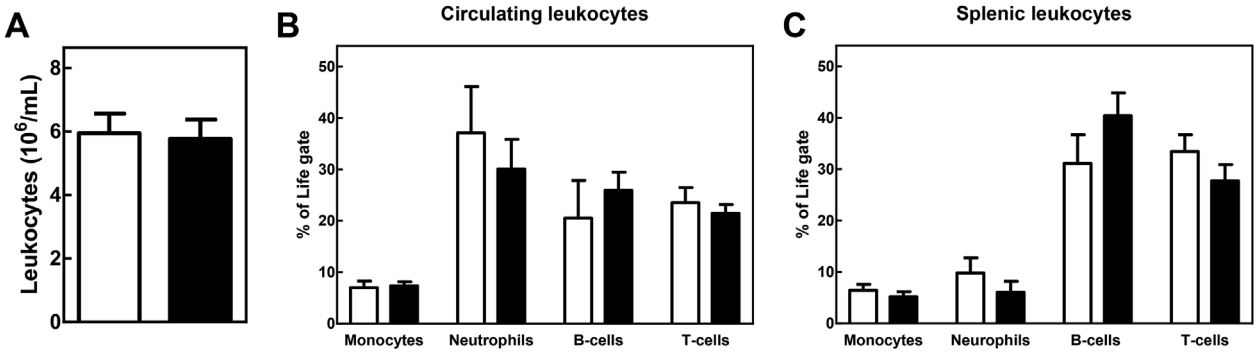

Fig. 6. Total leukocyte numbers and the distribution over leukocyte subpopulations are similar in *STAB1* KO and WT transplanted *LDLr* KO mice. (A) *STAB1* KO transplanted mice (black bar; N = 11) had similar total circulating leukocytes counts as WT transplanted mice (white bar; N = 12). (B) Bone marrow-specific deletion of *STAB1* (black bars; N = 6) did not affect the contribution of the individual leukocyte subpopulations as compared to WT transplanted control mice (white bars; N = 6) in the circulation or (C) in the spleen. Graphs represent means ± SEM.

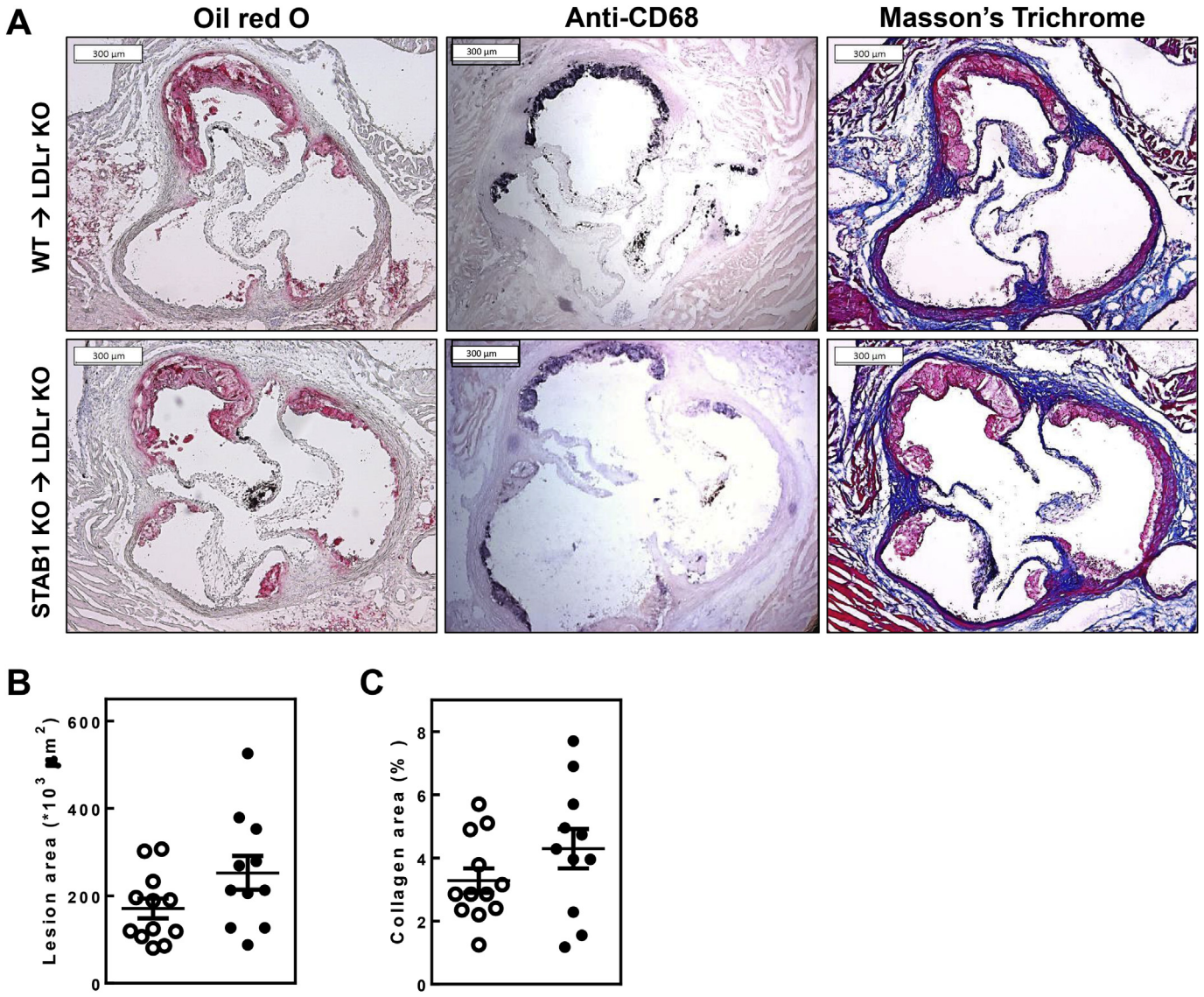

Fig. 7. Bone marrow-specific *STAB1* deletion in *LDLr* KO mice does not affect atherosclerotic lesion size or composition. (A) Representative micrographs of the aortic root stained with Oil red O for neutral lipids (*red*), anti-CD68 for macrophages (*black*) and Masson's Trichrome for collagen (*blue*) did not show a difference in the lesion size or composition between *STAB1* KO transplanted mice. (B) Atherosclerotic lesion area was not different in *STAB1* KO transplanted (black circles; N = 11) and WT transplanted (white circles; N = 12) *LDLr* KO mice after 9 weeks of Western-type diet feeding. (C) A similar percentage of collagen was measured in atherosclerotic lesions of both *STAB1* KO transplanted (black circles; N = 11) and WT transplanted (white circles; N = 12) *LDLr* KO mice. (For interpretation of the references to color in this figure legend, the reader is referred to the Web version of this article.)

marrow-specific deletion of *STAB1* did not translate into significant changes in the extent of *in vivo* foam cell formation. Furthermore, systemic lipid concentrations or circulating leukocytes were not altered as a result of bone marrow transplantation. Consequently, *STAB1* KO transplanted mice displayed a similar atherosclerosis susceptibility as compared to WT transplanted mice.

STAB2 exhibits a 55% homology in protein sequence with STAB1 [9]. Although the two receptors are related, the ligands of STAB1 and STAB2 are different. Whereas STAB1 mostly binds modified lipoproteins and SPARC, the major ligands for STAB2 include hyaluronan and AGE-modified proteins [4,29,30]. Schledzewski et al. showed that, despite the difference in ligands, both scavenger receptors are redundant as the individual single KO mice did not show major phenotypic changes while the double deficient mice died prematurely [31]. Hence, it cannot be excluded that absence of an effect of macrophage STAB1 deficiency on atherosclerosis susceptibility might be nullified by the presence of functional STAB2, especially since the presence of STAB2 has also been shown in subsets of macrophages and murine atherosclerotic lesions [32,33]. However important to note, we could not detect STAB2 in macrophage foam cells in our *in vitro* experimental set-up. To further investigate the hypothesis of STAB2 compensation for the loss of STAB1 in macrophages, the functional presence of STAB2 expressing macrophages in atherosclerotic lesions of *STAB1* KO transplanted mice needs to be established. Although endothelial progenitor cells can be derived from bone marrow, in our bone marrow transplantation atherosclerosis model we have never found any evidence of replacement of endothelial cells by cells from donor origin. However, STAB1 and STAB2 expression by the liver sinusoidal endothelial cells may be able to compensate for STAB1 deficiency in macrophages and may have distant effects on aortic atherosclerosis by controlling circulating ligands in the blood stream. It would therefore be valuable to compare the effects of STAB1/STAB2 single and double deficiency in total-body knockouts and in our bone marrow-specific model to investigate atherosclerotic lesion formation without the potentially confounding redundancy effects. Importantly, functional redundancy has also been shown for other macrophage scavenger receptors, i.e. SR-A1

and CD36. As such, the effects of deficiency of one or more scavenger receptors on atherosclerosis development in murine models is controversial and the conflicting outcomes are proposed to be dependent on the stage of the lesion development and the genetic make-up of the atherosclerotic background of the mice used for the experiment as reviewed by Moore and Freeman [34]. Here, we investigated STAB1 deficiency in initial lesions specifically. During our *in vitro* foam cell experiments, we observed a downregulation of STAB1 in foam cells of WT origin. Since STAB1 is virtually absent in WT cells after foam cell induction, we do not expect any macrophage-specific STAB1 effects on atherosclerotic lesion development in more advanced stages of the disease.

We observed an unexpected effect of bone marrow STAB1 deficiency on body weight development. Under healthy conditions, bone marrow-derived macrophages facilitate the turnover over adipocytes, but also influence lipolysis by producing catecholamines and play an essential buffering role during lipolysis of stored fats in adipocytes [35]. Moreover, in obesity, bone marrow-derived macrophages in adipose tissue play a key role [36,37]. Interestingly, the gene expression level of SPARC, a known ligand of STAB1, in the adipose tissue is increased in mouse models for obesity [38] and in obese humans [39]. In addition, the level of SPARC in the serum of patients with type 2 diabetes is increased independent of obesity [40]. Based upon these combined findings, it can be proposed that the increased adiposity observed in *STAB1* KO transplanted mice is not a direct effect of macrophage STAB1 deficiency but rather secondary to increased adipose tissue SPARC levels as a result of an inability of STAB1 knockout macrophages in adipose tissue to clear SPARC. It would be interesting to measure SPARC levels in adipose tissue to further investigate this hypothesis.

In conclusion, we have shown that macrophage STAB1 deficiency does not affect atherosclerosis susceptibility in *LDLr* KO mice. Notably, in addition to macrophages, STAB1 is expressed in murine aortic endothelial cells as well as human coronary arterial endothelial cells [5,13]. Given that in response to pathogens and modified lipoproteins endothelial cells can acquire a type II (pro-inflammatory) activation state [41,42], future research in total-body and endothelial cell-specific *STAB1* KO mice is warranted to potentially uncover a relevant contribution of endothelial STAB1 in the pathogenesis of atherosclerosis.

Conflicts of interest

The authors declare that they do not have anything to disclose regarding conflict of interest with respect to this manuscript.

Financial support

We acknowledge the support from the Netherlands CardioVascular Research Initiative: “the Dutch Heart Foundation, Dutch Federation of University Medical Centres, the Netherlands Organisation for Health Research and Development and the Royal Netherlands Academy of Sciences” for the GENIUS project “Generating the best evidence-based pharmaceutical targets for atherosclerosis” (CVON2011-19 to M.V.E.). This study was supported by the Netherlands Organization for Scientific Research (VICI Grant 91813603 to M.V.E.) and Dutch Heart Foundation grant 2012T080 awarded to M.H. M.V.E. is an Established Investigator of the Dutch Heart Foundation (Grant 2007T056).

Author contributions

J.E.N. performed experiments, analyzed and interpreted data and wrote the manuscript. M.H. designed and performed experiments, analyzed and interpreted data and aided in the preparation of the manuscript. S.V.H and J.J.G. performed experiments, interpreted data and aided in the preparation of the manuscript. C.M., S.G. and C.G. developed the murine models used in the experiment. M.V.E. conceived the experiments, interpreted data, supervised the study and provided financial support. All authors revised the manuscript and approved its final version.

Acknowledgements

We would like to thank P. van Santbrink and M.J. Kröner for their technical assistance during the experiments. Furthermore, we would like to thank I. Bot for providing the microarray data from the collar-induced lesion model for atherosclerosis.

References

[1] T.J.C. Van Berkel, R. Out, M. Hoekstra, J. Kuiper, E. Biessen, M. Van Eck, Scavenger receptors: friend or foe in atherosclerosis? Curr. Opin. Lipidol. 16 (5) (2005) 525–535, https://doi.org/10.1097/01.mol.0000183943.20277.26.

[2] S. Goerdt, L.J. Walsh, G.F. Murphy, J.S. Pober, Identification of a novel high molecular weight protein preferentially expressed by sinusoidal endothelial cells in normal human tissues, J. Cell Biol. 113 (6) (1991) 1425–1437.

[3] R. Li, A. Oteiza, K.K. Sørensen, P. Mccourt, R. Olsen, B. Smedsrød, et al., Role of Liver Sinusoidal Endothelial Cells and Stabilins in Elimination of Oxidized Low-density Lipoproteins vol. 33, (2011), pp. 71–81, https://doi.org/10.1152/ajpgi.00215.2010.

[4] J. Kzhyshkowska, G. Workman, M. Cardo-Vila, W. Arap, R. Pasqualini, A. Gratchev, et al., Novel function of alternatively activated macrophages: stabilin-1-mediated clearance of SPARC, J. Immunol. 176 (10) (2006) 5825–5832, https://doi.org/10.4049/jimmunol.176.10.5825.

[5] H. Adachi, M. Tsujimoto, FEEL-1, a novel scavenger receptor with in vitro bacteria-binding and angiogenesis-modulating activities, J. Biol. Chem. 277 (37) (2002) 34264–34270, https://doi.org/10.1074/jbc.M204277200.

[6] S.-Y. Park, M.-Y. Jung, S.-J. Lee, K.-B. Kang, A. Gratchev, V. Riabov, et al., Stabilin-1 mediates phosphatidylserine-dependent clearance of cell corpses in alternatively activated macrophages, J. Cell Sci. 122 (18) (2009) 3365–3373, https://doi.org/10.1242/jcs.049569.

[7] Y. Tamura, H. Adachi, J. Osuga, K. Ohashi, N. Yahagi, M. Sekiya, et al., FEEL-1 and FEEL-2 are endocytic receptors for advanced glycation end products, J. Biol. Chem. 278 (15) (2003) 12613–12617, https://doi.org/10.1074/jbc.M210211200.

[8] M. Karikoski, H. Irjala, M. Maksimow, M. Miiluniemi, K. Granfors, S. Hernesniemi, et al., Clever-1/Stabilin-1 regulates lymphocyte migration within lymphatics and leukocyte entrance to sites of inflammation, Eur. J. Immunol. 39 (2009) 3477–3487, https://doi.org/10.1002/eji.200939896.

[9] H. Adachi, M. Tsujimoto, FEEL-1, a novel scavenger receptor with in vitro bacteria-binding and angiogenesis-modulating activities, J. Biol. Chem. 277 (37) (2002) 34264–34270, https://doi.org/10.1074/jbc.M204277200.

[10] P. Rantakari, D.A. Patten, J. Valtonen, M. Karikoski, H. Gerke, H. Dawes, et al., Stabilin-1 expression defines a subset of macrophages that mediate tissue homeostasis and prevent fibrosis in chronic liver injury, Proc. Natl. Acad. Sci. Unit. States Am. 113 (33) (2016) 9298–9303, https://doi.org/10.1073/pnas.1604780113.

[11] S. Palani, M. Maksimow, M. Miiluniemi, K. Auvinen, S. Jalkanen, M. Salmi, Stabilin-1/CLEVER-1, a type 2 macrophage marker, is an adhesion and scavenging molecule on human placental macrophages, Eur. J. Immunol. 41 (7) (2011) 2052–2063, https://doi.org/10.1002/eji.201041376.

[12] S. Goerdt, R. Bhardwaj, C. Sorg, Inducible expression of MS-1 high-molecular-weight protein by endothelial cells of continuous origin and by dendritic cells/macrophages *in vivo* and in vitro, Am. J. Pathol. 142 (5) (1993) 1409–1422.

[13] I. Brochériou, S. Maouche, H. Durand, V. Braunersreuther, G. Le Naour, A. Gratchev, et al., Antagonistic regulation of macrophage phenotype by M-CSF and GM-CSF: implication in atherosclerosis, Atherosclerosis 214 (2) (2011) 316–324, https://doi.org/10.1016/j.atherosclerosis.2010.11.023.

[14] S. Mosig, K. Rennert, S. Krause, J. Kzhyshkowska, K. Neunubel, R. Heller, et al., Different functions of monocyte subsets in familial hypercholesterolemia: potential function of CD14 + CD16 + monocytes in detoxification of oxidized LDL, Faseb. J. 23 (3) (2009) 866–874, https://doi.org/10.1096/fj.08-118240.

[15] S. Palani, K. Elima, E. Ekholm, S. Jalkanen, M. Salmi, Monocyte stabilin-1 suppresses the activation of Th1 lymphocytes, J. Immunol. 196 (1) (2016) 115–123, https://doi.org/10.4049/jimmunol.1500257.

[16] E.M. Chu, D.C. Tai, J.L. Beer, J.S. Hill, Macrophage heterogeneity and cholesterol homeostasis: classically-activated macrophages are associated with reduced cholesterol accumulation following treatment with oxidized LDL, Biochim. Biophys. Acta Mol. Cell Biol. Lipids 1831 (2) (2013) 378–386, https://doi.org/10.1016/j.bbalip.2012.10.009.

[17] J. Oh, A.E. Riek, S. Weng, M. Petty, D. Kim, M. Colonna, et al., Endoplasmic reticulum stress controls M2 macrophage differentiation and foam cell formation, J. Biol. Chem. 287 (15) (2012) 11629–11641, https://doi.org/10.1074/jbc.M111.338673.

[18] W. Lee, S.Y. Park, Y. Yoo, S.Y. Kim, J.E. Kim, S.W. Kim, et al., Macrophagic stabilin-1 restored disruption of vascular integrity caused by sepsis, Thromb. Haemostasis 118 (10) (2018) 1776–1789, https://doi.org/10.1055/s-0038-1669477.

[19] A. Yurdagul Jr., A.C. Doran, B. Cai, G. Fredman, I.A. Tabas, Mechanisms and consequences of defective efferocytosis in atherosclerosis, Front Cardiovasc Med 4 (2018) 86, https://doi.org/10.3389/fcvm.2017.00086.

[20] M. Ackers-johnson, A. Talasila, A.P. Sage, X. Long, I. Bot, N.W. Morrell, et al., Myocardin regulates vascular smooth muscle cell inflammatory activation and

disease, Arterioscler. Thromb. Vasc. Biol. 35 (4) (2015) 817–828.
[21] J.H. Von Der Thüsen, T.J.C. Van Berkel, E.A.L. Biessen, Induction of rapid atherogenesis by perivascular carotid collar placement in apolipoprotein E – deficient and low-density lipoprotein receptor – deficient mice, Circulation (2001) 1164–1171.
[22] R. Out, M. Hoekstra, R.B. Hildebrand, J.K. Kruit, I. Meurs, Z. Li, et al., Macrophage ABCG1 deletion disrupts lipid homeostasis in alveolar macrophages and moderately influences atherosclerotic lesion development in LDL receptor-deficient mice, Arterioscler. Thromb. Vasc. Biol. 26 (10) (2006) 2295–2300.
[23] R. Out, W. Jessup, W. Le Goff, M. Hoekstra, I.C. Gelissen, Y. Zhao, et al., Coexistence of foam cells and hypocholesterolemia in mice lacking the ABC transporters A1 and G1, Circ. Res. 102 (1) (2008) 113–120.
[24] P. Chomczynski, N. Sacchi, Single-step method of RNA isolation by acid guanidinium extraction, Anal. Biochem. 162 (1987) 156–159.
[25] J.E. Nahon, M. Hoekstra, S.R. Havik, P.J. Van Santbrink, G.M. Dallinga-Thie, J.A. Kuivenhoven, et al., Proteoglycan 4 regulates macrophage function without altering atherosclerotic lesion formation in a murine bone marrow-specific deletion model, Atherosclerosis 274 (2018) 120–127, https://doi.org/10.1016/j.atherosclerosis.2018.05.008.
[26] F. Pucci, M.A. Venneri, D. Biziato, A. Nonis, D. Moi, A. Sica, et al., A distinguishing gene signature shared by tumor-infiltrating Tie2-expressing monocytes, blood "resident" monocytes, and embryonic macrophages suggests common functions and developmental relationships, Blood 114 (4) (2009) 901–914, https://doi.org/10.1182/blood-2009-01-200931.
[27] N.K. Schiller, N. Kubo, W.A. Boisvert, L.K. Curtiss, Effect of y-irradiation and bone marrow transplantation on atherosclerosis in LDL receptor – deficient mice, Arterioscler. Thromb. Vasc. Biol. 21 (10) (2001) 1674–1680.
[28] S.P. Weisberg, D. McCann, M. Desai, M. Rosenbaum, R.L. Leibel, A.W. Ferrante Jr., Obesity is associated with macrophage accumulation in adipose tissue, J. Clin. Invest. 112 (12) (2003) 1796–1808.
[29] J. Kzhyshkowska, A. Gratchev, H. Brundiers, S. Mamidi, L. Krusell, S. Goerdt, Phosphatidylinositide 3-kinase activity is required for stabilin-1-mediated endosomal transport of acLDL, Immunobiology 210 (2–4) (2005) 161–173, https://doi.org/10.1016/j.imbio.2005.05.022.
[30] B. Hansen, P. Longati, K. Elvevold, G.-I.I. Nedredal, K. Schledzewski, R. Olsen, et al., Stabilin-1 and stabilin-2 are both directed into the early endocytic pathway in hepatic sinusoidal endothelium via interactions with clathrin/AP-2, independent of ligand binding, Exp. Cell Res. 303 (1) (2005) 160–173, https://doi.org/10.1016/j.yexcr.2004.09.017.
[31] K. Schledzewski, C. Géraud, B. Arnold, S. Wang, H. Gröne, T. Kempf, et al., Deficiency of liver sinusoidal scavenger receptors stabilin-1 and -2 in mice causes glomerulofibrotic nephropathy via impaired hepatic clearance of noxious blood factors, J. Clin. Invest. 121 (2) (2011) 703–714.
[32] G.Y. Lee, J.H. Kim, G.T. Oh, B.H. Lee, I.C. Kwon, I.S. Kim, Molecular targeting of atherosclerotic plaques by a stabilin-2-specific peptide ligand, J. Contr. Release 155 (2) (2011) 211–217, https://doi.org/10.1016/j.jconrel.2011.07.010.
[33] S.Y. Park, M.Y. Jung, H.J. Kim, S.J. Lee, S.Y. Kim, B.H. Lee, et al., Rapid cell corpse clearance by stabilin-2, a membrane phosphatidylserine receptor, Cell Death Differ. 15 (1) (2008) 192–201, https://doi.org/10.1038/sj.cdd.4402242.
[34] K.J. Moore, M.W. Freeman, Scavenger receptors in atherosclerosis: beyond lipid uptake, Arterioscler. Thromb. Vasc. Biol. 26 (8) (2006) 1702–1711, https://doi.org/10.1161/01.ATV.0000229218.97976.43.
[35] L. Boutens, R. Stienstra, Adipose tissue macrophages: going off track during obesity, Diabetologia 59 (5) (2016) 879–894, https://doi.org/10.1007/s00125-016-3904-9.
[36] J.G. Neels, J.M. Olefsky, Inflamed fat: what starts the fire? J. Clin. Invest. 116 (1) (2006) 33–35.
[37] S. Weisberg, D. McCann, M. Desai, M. Rosenbaum, R. Leibel, A. Ferrante Jr., Obesity is associated with macrophage accumulation in adipose tissue, J. Clin. Invest. 112 (12) (2003) 1796–1808.
[38] S. Tartare-Deckert, C. Chavey, M.N. Monthouel, N. Gautier, E. Van Obberghen, The matricellular protein SPARC/osteonectin as a newly identified factor up-regulated in obesity, J. Biol. Chem. 276 (25) (2001) 22231–22237, https://doi.org/10.1074/jbc.M010634200.
[39] K. Kos, S. Wong, B. Tan, A. Gummesson, M. Jernas, N. Franck, et al., Regulation of the fibrosis and angiogenesis promoter SPARC/osteonectin in human adipose tissue by weight, Diabetes 58 (2009) 1780–1788, https://doi.org/10.2337/db09-0211 (August).
[40] D. Wu, L. Li, M. Yang, H. Liu, G. Yang, Elevated plasma levels of SPARC in patients with newly diagnosed type 2 diabetes mellitus, Eur. J. Endocrinol. 165 (4) (2011) 597–601, https://doi.org/10.1530/EJE-11-0131.
[41] J.S. Pober, W.C. Sessa, Evolving functions of endothelial cells in inflammation, Nat. Rev. Immunol. 7 (10) (2007) 803–815, https://doi.org/10.1038/nri2171.
[42] J.S. Pober, R.S. Cotran, Cytokines and endothelial cell biology, Physiol. Rev. 70 (2) (1990) 427–451.